Aerogravity evidence for major crustal thinning under the Pine Island Glacier region (West Antarctica)

T.A. Jordan[1,†], F. Ferraccioli[1], D.G. Vaughan[1], J.W. Holt[2], H. Corr[1], D.D. Blankenship[2], and T.M. Diehl[2]
[1]*British Antarctic Survey, High Cross, Madingley Road, Cambridge, CB3 0ET, UK*
[2]*University of Texas, Institute of Geophysics, 10100 Burnet Road, Austin, Texas 78758-4445, USA*

ABSTRACT

The West Antarctic Rift System provides critical geological boundary conditions for the overlying West Antarctic Ice Sheet. Previous geophysical surveys have traced the West Antarctic Rift System and addressed the controls that it exerts on the West Antarctic Ice Sheet in the Ross Sea Embayment. However, much less is known about the rift system under the Amundsen Sea Embayment, a key sector of the West Antarctic Ice Sheet, which is thinning significantly today. New aerogravity data over the Pine Island Glacier region, one of the fastest flowing glaciers within the Amundsen Sea Embayment, sheds new light into the crustal structure under this dynamic part of the West Antarctic Ice Sheet. Three-dimensional (3-D) inversion of terrain-decorrelated free-air and Bouguer gravity anomaly data reveal significant crustal thinning beneath the catchment of Pine Island Glacier. Under the Byrd Subglacial Basin and the newly identified Pine Island Rift, Moho depth is estimated to be 19 ± 1 km. This is the thinnest crust observed beneath the West Antarctic Ice Sheet. Estimates of lithosphere rigidity (T_e), based on isostatic models, yield a T_e of 5 ± 5 km, which is comparable to values from modern rift systems such as the Basin and Range Province. Major crustal thinning, coupled with low lithosphere rigidity, attest to the considerable impact of continental rifting beneath this part of the West Antarctic Ice Sheet. In analogy with the better known Ross Sea segment of the West Antarctic Rift System we suggest that the Amundsen Sea Embayment was affected by distributed Cretaceous rifting, followed by Cenozoic narrow-mode rifting. Narrow-mode rifting within the Pine Island Rift is particularly important as it may serve as a geological template for enhanced glacial flow associated with Pine Island Glacier.

[†]E-mail: tomj@bas.ac.uk

INTRODUCTION

The West Antarctic Rift System (Fig. 1) is thought to extend from the Ross Sea to the Bellingshausen Sea and has been compared to other major continental rift zones, such as the Basin and Range Province or the East African Rift System (LeMasurier and Thomson, 1990; LeMasurier and Landis, 1996; Winberry and Anandakrishnan, 2003; LeMasurier, 2008). While the Ross Sea segment of the West Antarctic Rift System is relatively well understood, due to extensive seismic and potential-field exploration (Damaske et al., 1994; Brancolini et al., 1995; Behrendt, 1999) coupled with drilling (Cape-Roberts-Science-Team, 2000; Fielding et al., 2006), a greater degree of uncertainty surrounds the reminder of the rift system. The reasons for this are that it is obscured by the West Antarctic Ice Sheet and that current geophysical surveys do not provide comprehensive coverage (Dalziel, 2006).

The location of the West Antarctic Rift System beneath the West Antarctic Ice Sheet is highly significant because bedrock geology, and the crustal structure of the rift system, may influence the dynamics of the overlying glaciers, which in turn affect the stability of the ice sheet (Dalziel and Lawver, 2001; Rignot et al., 2008). The suggestion that the rift system may provide critical boundary conditions on ice dynamics is supported by geophysical studies over the Ross Sea Embayment sector of the West Antarctic Rift System. For example, airborne geophysics revealed a rift basin with sedimentary infill under the onset region of Ice Stream B (Bell et al., 1998). Airborne radar and aeromagnetic investigations have led to the suggestion that active or recently active subglacial volcanism associated with the West Antarctic Rift System may also promote enhanced glacial flow by increasing the availability of water beneath the Ross Sea Embayment region (Blankenship et al., 1993; Hulbe and MacAyeal, 1999; Vogel and Tulaczyk, 2006).

Recent studies show that parts of the West Antarctic Ice Sheet are thinning, with the most dramatic changes occurring in the Amundsen Sea Embayment (Davis et al., 2005). Pine Island Glacier is one of the fastest flowing glaciers in the Amundsen Sea Embayment (Fig. 2) and is thinning and retreating rapidly, contributing to accelerated global sea-level rise (Rignot, 1998; Shepherd et al., 2004; Thomas et al., 2004). However, the geological boundary conditions for this highly dynamic part of the West Antarctic Ice Sheet remain poorly constrained (Ferraccioli et al., 2007), despite the availability of subice information from recent radio echo sounding and gravity data (Holt et al., 2006a; Vaughan et al., 2006; Diehl et al., 2008).

Here we focus on utilizing newly acquired airborne gravity data to model the crustal structure of the West Antarctic Rift System beneath the catchment of Pine Island Glacier (Fig. 2). A variety of 3-D inversion techniques provide new estimates of crustal thickness under this poorly known sector of the West Antarctic Rift System. In addition, we compare the observed gravity data with local and regional isostatic compensation models to derive the rigidity of the rifted lithosphere (T_e). Our crustal models for the Amundsen Sea Embayment region reveal the occurrence of multiple continental rifting stages, including wide-mode Cretaceous rifting, followed by narrow-mode Cenozoic rifting. We suggest that the latter rifting stage may be of significant relevance for enhanced glacial flow associated with Pine Island Glacier.

GEOLOGICAL AND GEOPHYSICAL SETTING

Cretaceous rifting within the West Antarctic Rift System is thought to have been caused by ridge-trench collision and progressive westerly cessation of subduction along the paleo-Pacific margin of Gondwana between 110 and 94 Ma (Mukasa and Dalziel, 2000; Larter et al., 2002). This passive rifting event may have led to the eventual separation of New Zealand and Chatham Rise from Antarctica ca. 85 Ma (Luyendyk, 1995). Alternatively, the early rift

GSA Bulletin; May/June 2010; v. 122; no. 5/6; p. 714–726; doi: 10.1130/B26417.1; 8 figures; 1 table.

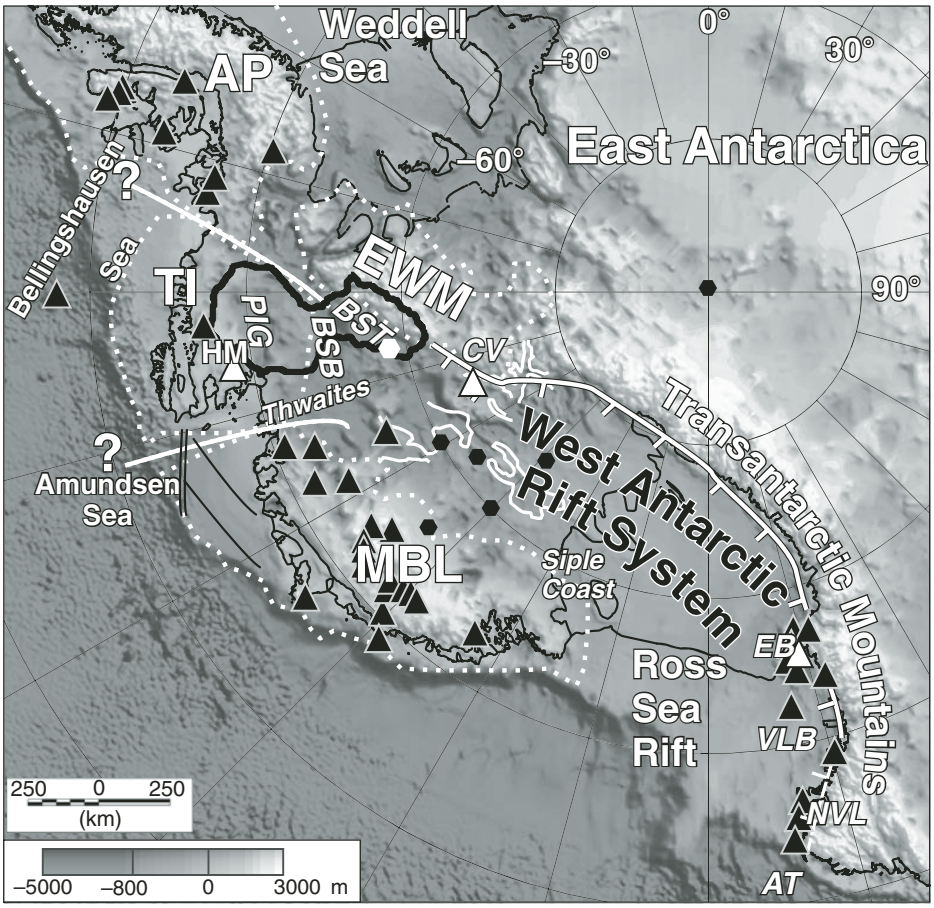

Figure 1. Regional tectonic sketch map showing the crustal setting of West Antarctica and the Pine Island Glacier (PIG) aerogeophysical survey area, overlaid on bedrock elevations derived from BEDMAP (Lythe et al., 2000). The outline of the PIG catchment is traced in black. Tectonic blocks from Dalziel and Elliot (1982) in dotted white, namely: AP—Antarctic Peninsula, EWM—Ellsworth-Whitmore Mountains, TI—Thurston Island block, MBL—Marie Byrd Land. Possible extensions of the West Antarctic Rift System into the Amundsen or the Bellingshausen Sea Embayments are thick white lines (Dalziel, 2006). Sedimentary basins inferred within the West Antarctic Rift System from previous aerogeophysical surveys are shown in thin white and are taken from Bell et al. (2006). Triangles mark Cenozoic volcanoes (LeMasurier and Thomson, 1990). Black triangles show inactive volcanoes and white triangles are recently active ones. Abbreviations as follows: EB—Mount Erebus; CV—Mount CASERTZ, subglacial volcano; HM—Hudson Mountains; Victoria Land Basin (VLB); NVL—Northern Victoria Land; AT—Adare Trough; BSB—Byrd Subglacial Basin; BST—Bentley Subglacial Trench. Black lines offshore PIG mark geophysical features associated with ca. 90 Ma rifting, and deformation along the margin of the Bellingshausen Plate 79–61 Ma (Gohl et al., 2007). Black hexagons—location of passive seismic stations (Winberry and Anandakrishnan, 2004); white hexagon is the only passive seismic station within our aerogeophysical survey area.

stage may have been actively driven by a Cretaceous mantle plume centered beneath Marie Byrd Land (Weaver et al., 1994).

Further evidence for Cretaceous intracontinental extension is seen in mylonitic gneisses dredged from the eastern Ross Sea Rift, which yield deformation ages of 98–95 Ma. These rocks also yield U-Pb zircon emplacement ages of 102–97 Ma, which can be correlated onshore to the A-type Byrd Coast Granite, which is related to continental extension (Siddoway et al., 2004). On the Marie Byrd Land coast mafic magmatism occurred at ca. 107 Ma and may be linked to the presence of a mantle plume (Storey et al., 1999). Structural evidence in the Ford Ranges suggests Cretaceous transtensional rifting (Siddoway et al., 2005), and aeromagnetic patterns indicate subglacial Cretaceous mafic magmatism and block faulting on the Edward VII Peninsula (Ferraccioli et al., 2002). Further to the east, offshore from Pine Island Glacier, two geophysical features are identified, thought to be associated with ca. 90 Ma rifting and later deformation along the margin of the Bellingshausen Plate between 79 and 61 Ma (Fig. 1) (Gohl et al., 2007).

After the initial Cretaceous phases of rifting there appears to have been a period of tectonic quiescence in Marie Byrd Land leading to the development of a low-relief erosion surface around 85–75 Ma (LeMasurier and Landis, 1996). Rift-related alkaline magmatism began at ca. 50 Ma in Northern Victoria Land (Fig. 1) (Rocchi et al., 2002). However, in Marie Byrd Land the oldest Cenozoic intrusive magmatism is ca. 34 Ma (Rocchi et al., 2006), and the main phase of volcanism began at 28–30 Ma (LeMasurier and Thomson, 1990). Pliocene and recently active volcanism in Marie Byrd Land and the Ross Sea region has continued to the present-day (LeMasurier and Thomson, 1990). In the Hudson Mountains, on the southeastern edge of the Thurston Island block (Fig. 1), outcrops of Late Miocene and Pliocene subaerial basaltic lavas and hyaloclastites are also observed (LeMasurier and Thomson, 1990). There is also evidence of recent (ca. 2 ka) volcanism in the Hudson Mountains, based on interpretation of a bright reflector within the ice, identified from new airborne radar data (Corr and Vaughan, 2008).

Evidence for extensive magmatism of inferred Cenozoic age beneath the West Antarctic Ice Sheet derives mainly from aeromagnetic data (Behrendt et al., 1996). This volcanism could be linked to oceanic rifting in the Adare Trough (Cande et al., 2000), which has been directly linked to continental rifting and magmatism within the Ross Sea Rift (Davey et al., 2006). Alternatively Cenozoic magmatism may relate to transtension in the Ross Sea Rift region (Ferraccioli et al., 2000; Rocchi et al., 2002). However, the widely distributed Cenozoic magmatism beneath the West Antarctic Ice Sheet is unlikely to result solely from far-field rifting or transtensional processes localized within the Ross Sea Rift. A Cenozoic mantle plume underlying some or all of the West Antarctic Rift System has been proposed by several authors (Behrendt et al., 1996; Behrendt, 1999; Storey et al., 1999). The presence of a plume explains the geochemical signatures and the generation of such large volumes of Cenozoic magmatism and is not in disagreement with the modest intraplate Cenozoic

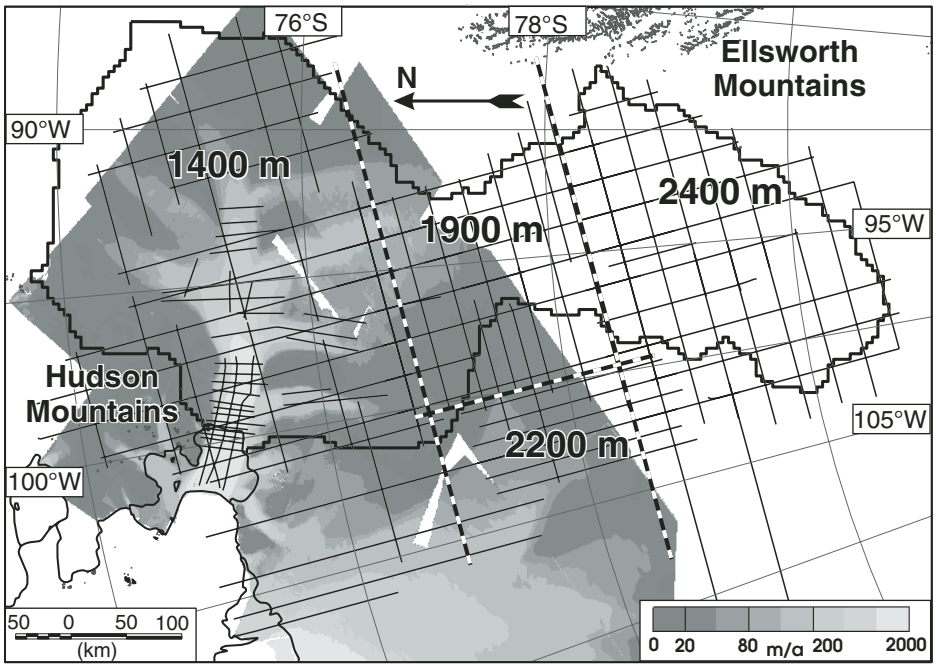

Figure 2. Ice velocity derived from InSAR data (Rignot et al., 2004) across the catchment of the Pine Island Glacier (black outline). Thin black lines mark our aerogeophysical survey flight lines. Dashed black and white lines separate different survey blocks and the bold numbers indicate the respective flight elevations. Dark gray outlines mark rock outcrops.

crustal extension in West Antarctica predicted by some plate-tectonic reconstructions (Lawver and Gahagan, 1994; Steinberger et al., 2004). However, an alternate hypothesis invokes the existence of a diffuse alkaline magmatic province linked to detachment in Eocene times of late Cretaceous subducted slabs (Finn et al., 2005).

Major debate centers on the relative amount of Cenozoic extension in West Antarctica. Marine geophysical evidence over the Adare Trough suggest ~180 km of extension between 43 and 26 Ma (Cande et al., 2000). There is little evidence for major subsequent structural activity in the Adare Trough indicating that this part of the West Antarctic Rift system became largely inactive in the early Miocene (Müller et al., 2005). Extension within the Adare Trough may link, via intracontinental transfer faulting, to continental rifting in the western Ross Sea Rift (Davey et al., 2006). Alternatively Cenozoic crustal extension may be more diffuse and may have also affected the Central and Eastern basins of the Ross Sea Rift (Decesari et al., 2007). Comparison between the subice topography of the West Antarctic Rift System and other major rift systems has led to the suggestion that Neogene rifting may have affected the Byrd Subglacial Basin and the Bentley Subglacial Trench (LeMasurier, 2008).

It is unclear if parts of West Antarctic Rift System are currently active or not (Dalziel, 2006). A single magnetotelluric experiment within the Byrd Subglacial Basin (Fig. 1) suggests that, at least locally, the lower crust and upper mantle of the West Antarctic Rift System has much higher resistivity, compared to other modern rift systems (Wannamaker et al., 1996). Low earthquake magnitude and localized distribution of seismic events beneath the West Antarctic Rift System, compared to other major active continental rifts, also suggests that there may be limited active rifting (Winberry and Anandakrishnan, 2003).

SURVEY DESIGN AND DATA REDUCTION

The British Antarctic Survey conducted an airborne geophysical survey during the 2004–2005 field season over the Pine Island Glacier catchment area (Fig. 2). A relatively coarse line and tie line spacing (~30 km) was selected to enable, together with the U.S.-led AGASEA aerogeophysical survey, reconnaissance mapping of subglacial topography, geology, and ice-sheet structure across the entire Amundsen Sea Embayment in a single field season (Fig. 3A) (Holt et al., 2006a; Vaughan et al., 2006). Our survey produced ~30,000 line-km of new airborne gravity data. In addition, a detailed draped airborne radar and aeromagnetic survey was flown, over the fast-flowing trunk of Pine Island Glacier (Fig. 2). Airborne gravity data were not collected on this higher resolution survey because of the vertical accelerations associated with draped flying.

The regional gravity survey was flown in four constant elevation blocks (Fig. 2). This survey design resulted in a minimum ground clearance, important for recovery of high-quality radar and magnetic data, without changing altitude within a block. Aircraft altitude changes, which produce higher accelerations and make recording accurate gravity data difficult, were restricted to turns at the end of lines. The Twin Otter aircraft used for the survey generally flew at ~60 m/s along the flight lines and completed the survey in a series of ~1000-km sorties. An overlap of ~30 km of level flight was allowed across survey block boundaries to ensure continuous coverage of useable gravity data. Additionally overlapping lines allowed for removal of filtering artifacts at the ends of lines (Bell et al., 1999).

Airborne gravity data were collected using LaCoste and Romberg air-sea gravimeter S-83 (LaCoste, 1967), modified and updated by the Zero Length Spring Corporation. The meter was mounted in a gyro-stabilized, shock-mounted platform, close to the center of mass of the aircraft to minimize the detrimental effect of vibrations and rotational motions on the meter. The meter platform operated with a 4 min period, yielding an acceptable trade-off between damping of horizontal accelerations and time required for the platform to stabilize (Valliant, 1992).

All the sorties started and ended at the same field camp and tie-down location (77°34.2′ S, 95°55.7′ W). Absolute gravity readings at this location were independently tied to absolute base stations at Rothera Station (Jones and Ferris, 1999) and McMurdo Station (Sasagawa et al., 2004) using LaCoste and Romberg land gravity meters (Diehl et al., 2008). The tie from Rothera gave a value of 982,446.0373 mGal at the Pine Island field camp, while the tie from McMurdo (via a field camp on Thwaites Glacier) gave a value of 982,446.682 mGal. The relative mismatch between the ties is significantly less than the typical accuracies for an airborne gravity survey (Bell et al., 1999). The McMurdo tie was preferred as there was less time between observations at the Thwaites and Pine Island field camps than between observations at Rothera and the Pine Island camp.

Standard processing steps were taken to convert the raw airborne gravity data to free-air anomalies (Jones and Johnson, 1995; Jones et al., 2002; Ferraccioli et al., 2005; Ferraccioli et al., 2006; Jordan et al., 2007). This included

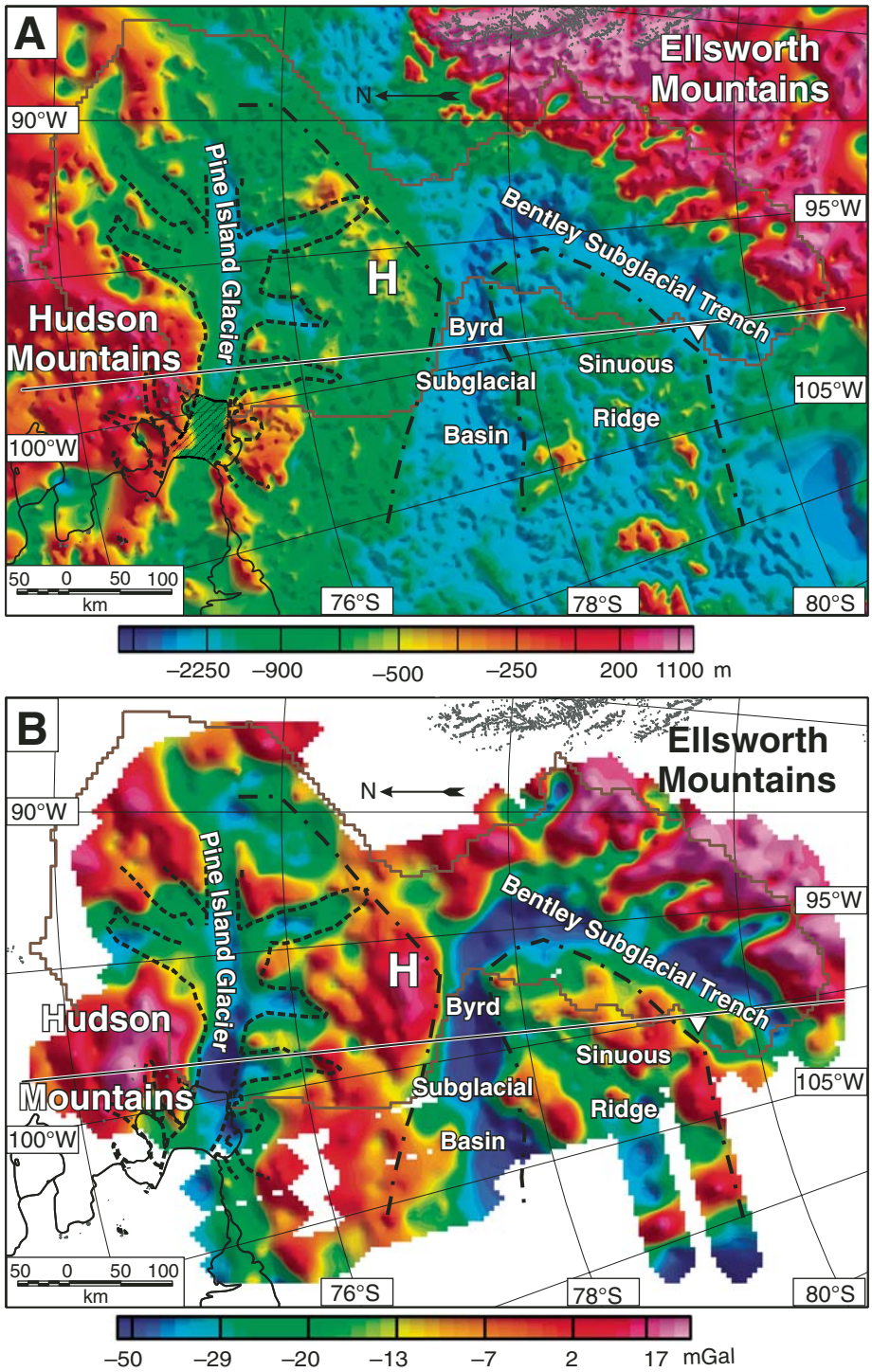

Figure 3. (A) Subglacial topography beneath the catchment of Pine Island Glacier (brown), modified from Vaughan et al. (2006) and Holt et al. (2006a). Dot-dash line marks major topographic discontinuities between subglacial highlands on the southern side of Pine Island Glacier (H) and the Byrd Subglacial Basin, and between the Sinuous Ridge and the Bentley Subglacial Trench. White triangle marks location of passive seismic station (Winberry and Anandakrishnan, 2004). The hashed region at the mouth of Pine Island Glacier, between the ice front and the grounding line, is where bed topography is unconstrained by radar data. (B) Free-air gravity anomaly map with superimposed topographic boundaries. In this and following figures a dashed black outline marks the region of fast flow associated with Pine Island Glacier. Labels as above.

making latitude, free-air, vertical acceleration, and Eötvös corrections (Harlan, 1968; Woollard, 1979) based on differential, carrier-phase, kinematic global positioning system (GPS) positional data (Mader, 1992). In addition to the standard processing steps, mentioned previously, a correction was made for gravimeter reading errors caused by the platform tilting, when it was subjected to horizontal accelerations (Swain, 1996).

The raw free-air gravity anomaly remains dominated by short-wavelength noise even after removal of all dynamic corrections (Bell et al., 1999; Jordan et al., 2007). Filtering is therefore required to minimize the residual short-wavelength noise. Two filters were considered: a standard fast-Fourier transform-based Butterworth filter (with a 7.5-km half-width) and a space-domain kernel filter (with a 9-km half-width), developed by the University of Texas (Holt et al., 2006b). Both filters gave similar results along the line. However, there was a significant problem with "ringing" of the Butterworth filter close to the end of the lines. The space-domain filter was therefore preferred. The filtered free-air gravity data were upward continued (Blakely, 1995) to a constant level of 2400 m. The final free-air gravity data were gridded using a tensioned spline technique (Smith and Wessel, 1990) with a tension factor of 0.25 and grid mesh of 5 km (Fig. 3B). The overall quality of the new airborne gravity data is high with a standard deviation for 265 crossover points of 2.8 mGal. Despite the lack of leveling these crossover errors are comparable to those reported for previous airborne gravity surveys over West and East Antarctica (Bell et al., 1999; Jones et al., 2002; Ferraccioli et al., 2005; Ferraccioli et al., 2006).

We calculated the complete Bouguer correction from the regional topographic grids, which included all available onshore and offshore regional data (Holt et al., 2006a; Vaughan et al., 2006). The Bouguer correction was calculated at the 2400 m observation altitude using a 3-D Gauss-Legendre quadrature (GLQ) method (von Frese et al., 1981). The topographic grids included data extending at least 165 km from the gravity flights, allowing the computation of a fully terrain-corrected Bouguer gravity anomaly (i.e., equivalent to Hayford zone O). The gravity effects of ice and water were calculated assuming densities of 915 and 1028 kg m^{-3}, respectively. The rock (topographic) correction used a standard density of 2670 kg m^{-3}. Bedrock topography above 0 m (as defined by the WGS84 ellipsoid) gave a positive gravity effect and bedrock topography below 0 m gave a negative gravity effect. The summation of the ice, water, and topographic gravity effects gave the total terrain gravity effect. Subtraction of the

terrain gravity effect from the free-air anomaly yielded the complete, terrain-corrected, Bouguer gravity anomaly. The Bouguer anomalies were then gridded using the same technique as the free-air data (Fig. 4A).

AEROGEOPHYSICAL IMAGES

Bedrock Topography and Free-Air Gravity Anomaly Maps

The subice topography (Fig. 3A) and new free-air gravity anomaly (Fig. 3B) show, as expected, a high degree of correlation. The Ellsworth Mountains are over 4000 m high and are associated with positive free-air gravity anomalies of up to 60 mGal, in contrast to prominent free-air gravity lows over the Bentley Subglacial Trench, Byrd Subglacial Basin, and Pine Island Glacier. The Bentley Subglacial Trench is ~2200 m deep and is separated from the broader Byrd Subglacial Basin by a region of elevated, but highly dissected, topography, referred to as Sinuous Ridge (Holt et al., 2006a). Between the Byrd Subglacial Basin and Pine Island Glacier there is also a region of elevated topography, which is less dissected than the Sinuous Ridge (H in Fig. 3A).

Pine Island Glacier flows in a confined subglacial valley up to 1600 m deep. The morphology of this deep valley suggests that the glacier may flow in a graben-like feature. In contrast, the elevated Hudson Mountains lie along the northern flank of Pine Island Glacier and feature positive free-air anomalies of up to ~50 mGal. The Hudson Mountains contain several Cenozoic basaltic volcanoes (LeMasurier and Thomson, 1990).

Bouguer Gravity Anomaly Map

The Bouguer gravity anomaly map (Fig. 4A) reveals a prominent long-wavelength negative anomaly over the Ellsworth Mountains between –20 and –104 mGal, which we interpret as evidence for thick crust. The inferred rift flank (Fitzgerald and Stump, 1991) between the Ellsworth Mountains block and the West Antarctic Rift System is marked by a prominent NE-SW oriented Bouguer anomaly gradient (L1 in Fig. 4A). Over the Hudson Mountains the regional Bouguer gravity anomaly is between –40 and –10 mGal, which may also reflect relative crustal thickening. A discrete, ~20 mGal, positive Bouguer anomaly (A) over the Hudson Mountains is associated with outcrops of Cenozoic basaltic volcanic rocks (LeMasurier and Thomson, 1990) and is likely to arise from dense mafic intrusions associated with Cenozoic to Holocene (Corr and Vaughan, 2008) volcanism. Regional positive Bouguer anomalies

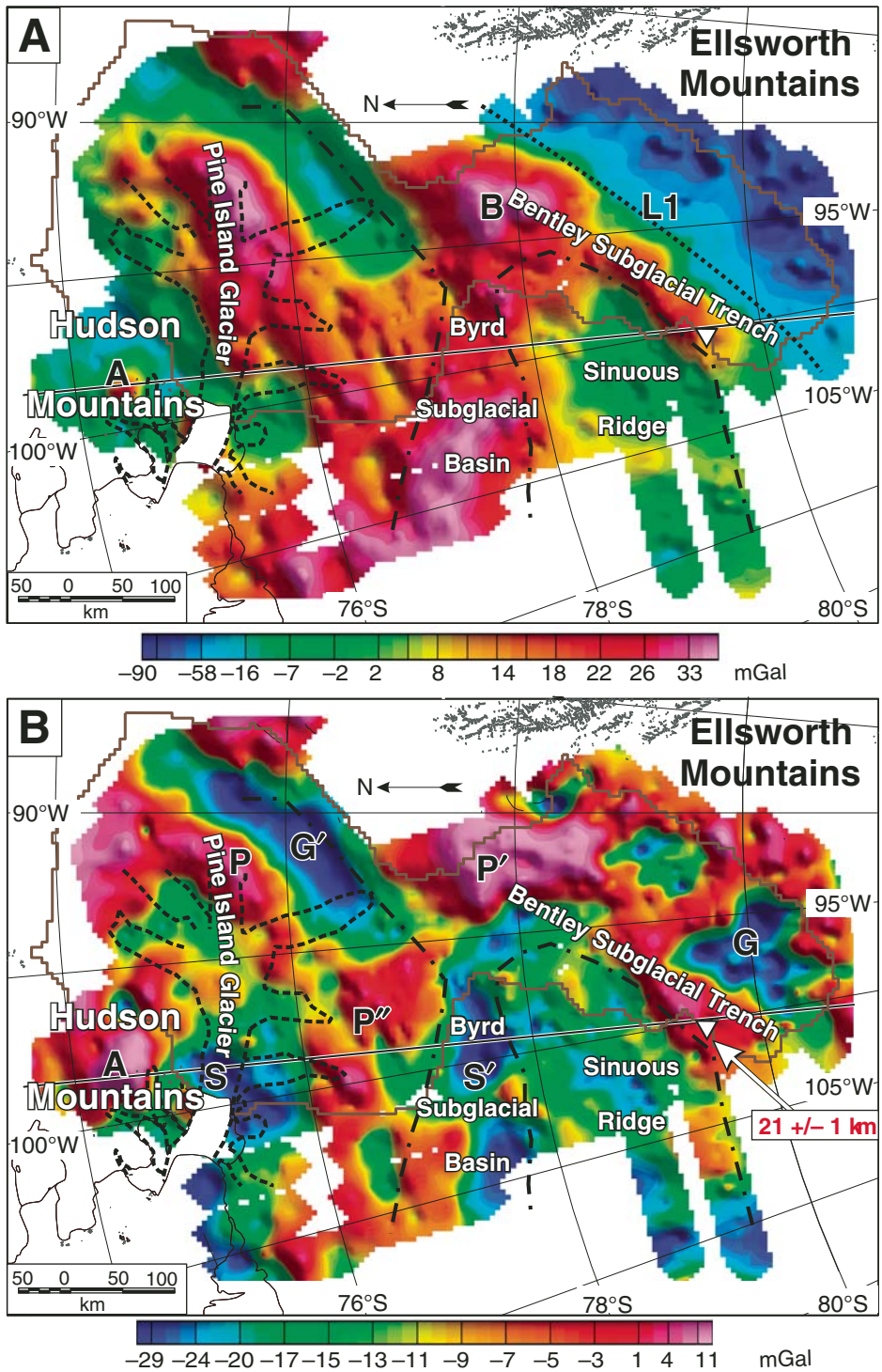

Figure 4. (A) Bouguer gravity anomaly map. Note data between grounding line and ice front has been excluded because of the lack of bathymetry data. (B) Airy isostatic anomaly map, assuming crustal and mantle densities of 2800 and 3330 kg m^{-3}, respectively. Boxed red number shows Moho depth and associated error estimate recovered at the seismic station of Winberry and Anandakrishnan (2004), which was used as a reference value to model regional Moho undulations from our new aerogravity data. Letters mark features referred to in the text. Black line marks cross section shown in Figures 5 and 8.

overlie the eastern segment of Pine Island Glacier, the Byrd Subglacial Basin, and the Bentley Subglacial Trench.

Airy Isostatic Anomaly Map

To provide an initial assessment of the intracrustal structure across the survey area, we calculated the gravity anomaly due to Airy isostatic compensation of the known surface loads (i.e., subglacial topography and ice thickness). To calculate the gravity effect of isostatic compensation a reference Moho depth must be assumed. Using a reference Moho depth of 23 km yields a predicted Airy isostatic Moho in the Bentley Subglacial Trench within 500 m of the independent receiver function estimate (Winberry and Anandakrishnan, 2004).

The Airy isostatic residual anomaly map (Fig. 4B) is obtained by subtracting the Airy model from the Bouguer anomaly. The regional negative Bouguer anomaly over the Ellsworth Mountains is now effectively removed, suggesting that this region is close to being in isostatic equilibrium. Negative isostatic residual anomalies (S and S′ in Fig. 4B) over the coastal part of Pine Island Glacier and over the Byrd Subglacial Basin may represent the gravity signature of thick sedimentary basins. The interpretation of sedimentary infill within the Byrd Subglacial Basin is supported by airborne radar data that shows the bedrock in the basin is remarkably smooth. The negative isostatic anomalies within the Ellsworth Mountains (G) and southeast of the Pine Island Glacier (G′) are associated with elevated and rougher topography, and may arise from uplifted low-density sedimentary rocks or granitoids.

Positive Airy isostatic anomalies mark the eastern end of Pine Island Glacier (P) and the Bentley Subglacial Trench (P′) and could imply thinner crust than predicted by the Airy isostatic model, or dense intrusions associated with subglacial volcanism. The short-wavelength character of the anomalies favors the latter hypothesis. In the Hudson Mountains the positive Bouguer anomaly (A) is enhanced by the Airy isostatic correction to over 28 mGal, supporting our interpretation of a dense mafic intrusion in this region. Between Pine Island Glacier and the Byrd Subglacial Basin there is a region of small-amplitude positive Airy isostatic residual anomalies (P″), between –2 and 11 mGal, which may also reveal dense rift-related mafic rocks.

Gravity Signatures along a Profile across the West Antarctic Rift System

We extracted a cross section across the Pine Island Glacier region to show the relationship between subice topography, free-air gravity, and Bouguer and Airy isostatic anomalies (Fig. 5). The profile was chosen so as to cross the main subglacial basins, which we interpret as being part of the West Antarctic Rift System and the flanking elevated topography of the Hudson and Ellsworth Mountains. In addition, our cross section intersects the only available seismic station over this part of the West Antarctic Rift System (Winberry and Anandakrishnan, 2004). Positive Bouguer gravity anomalies are detected over Pine Island Glacier, Byrd Subglacial Basin, and the Bentley Subglacial Trench. The Airy anomalies show differing signatures over the basins. Both the Pine Island Glacier and the Byrd Subglacial Basin exhibit prominent lows, while the Bentley Subglacial Trench features a high. The subice topography (Fig. 5A) suggests that these basins may be graben- or half-graben-like structures and the Airy isostatic signature would be consistent with the presence of sedimentary infill in part of Pine Island graben and Byrd Subglacial Basin. In contrast, the high over the Bentley Subglacial Trench would suggest thin sedimentary infill, consistent with independent seismic evidence for less than 500-m infill (Winberry and Anandakrishnan, 2004). To further our understanding of the source of the positive Bouguer anomalies over the newly identified grabens we estimated the rigidity of the lithosphere and the crustal thickness variations within this part of the West Antarctic Rift System.

ESTIMATING LITHOSPHERE RIGIDITY (T_e)

The Airy isostatic model we presented assumes that the lithosphere has no lateral strength. However, the response of the lithosphere to loads is better approximated as an elastic plate with an equivalent thickness referred to as T_e (Watts, 2001). Because the rigidity of the West Antarctic Rift may have increased with time after rifting, in a similar manner to the oceanic lithosphere (Watts, 2001), estimates of the timing of rifting can also be made by analyzing T_e (Karner et al., 2005).

We adopt the method of Stewart and Watts (1997) to assess the elastic thickness for this sector of the West Antarctic Rift System assuming that compensation of the ice and topographic loads occurs at the Moho. We determined the best-fitting regional T_e by comparing calculated gravity anomalies from different isostatic models with the observed Bouguer anomaly (Fig. 6). We chose to apply the simplest possible model of isostatic compensation, where load density (ρ_{load}) = crustal density (ρ_{crust}) (Stewart and Watts, 1997). We also used parameters comparable to those of Stewart and Watts (1997), where a Young's modulus of 10^{11} Pa and a Poisson's ratio of 0.25 define the properties of the elastic beam, and ρ_{load} = 2670 kg m^{-3} and mantle density (ρ_{man}) = 3330 kg m^{-3}. The ice thickness and offshore water depth were converted into equivalent rock thickness (assuming ρ_{ice} = 915 kg m^{-3} and ρ_{water} = 1028 kg m^{-3}) and added to the elevation of the subice topography. Three-dimensional undulations in the isostatic compensating surface were calculated for all grid points simultaneously using a fast Fourier transform routine, grdfft, a component of the

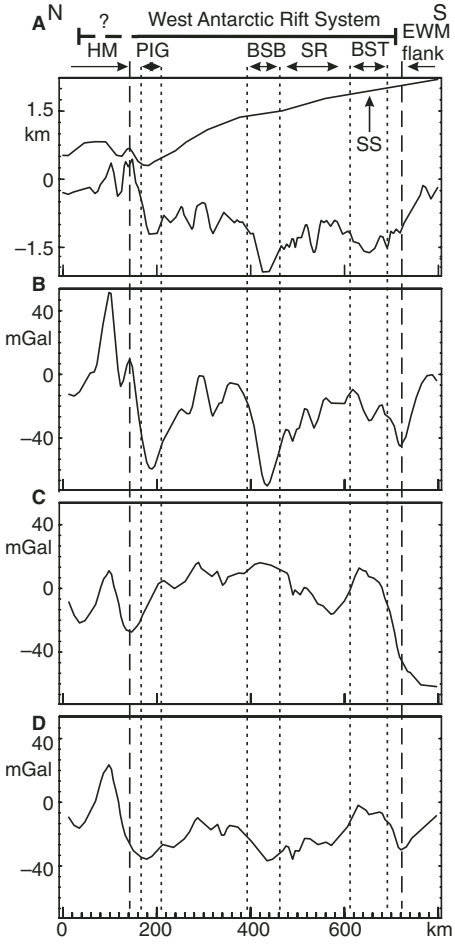

Figure 5. Cross-section view across the West Antarctic Rift System underlying the Pine Island Glacier catchment and corresponding gravity signatures. EWM—Ellsworth-Whitmore Mountains; SS—seismic station (Winberry and Anandakrishnan, 2004), SR—Sinuous Ridge, other abbreviations as in Figure 1. (A) Subglacial topography of the rift basins and uplifted flanks. Note the graben-like basin underlying Pine Island Glacier. (B) Free-air gravity anomalies across the rifted region. (C) Bouguer gravity anomalies and (D) Airy isostatic anomalies. See text for detailed description.

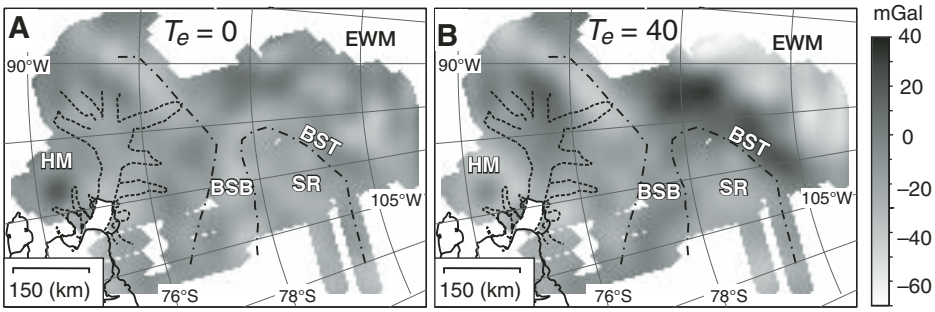

Figure 6. Comparison between end member isostatic models for this part of the West Antarctic Rift System. Note the higher amplitude residuals in panel B referring to the higher rigidity model (T_e = 40) compared to the Airy model (T_e = 0) shown in panel A.

GMT software package (Wessel and Smith, 1991). Isostatic models for constant T_e values of between 0 and 40 km were constructed and the gravity field for each model calculated using the GLQ program (von Frese et al., 1981) for a reference Moho depth of 23 km and an observation altitude of 2400 m.

In Figure 6 we analyzed the spatial distribution of residuals calculated as the difference between the observed Bouguer gravity anomaly and the isostatic models for the two end-member models of T_e = 0 and T_e = 40. The low T_e models over this sector of the West Antarctic Rift System yield an improved fit to the observed data (standard deviation of 10 mGal for T_e = 0) compared to the higher T_e models (standard deviation of 20 mGal for T_e = 40 km). The best-fit isostatic model was obtained for a T_e of (5 ± 5 km), which yielded standard deviations of ~9 mGal.

The Pine Island Glacier graben, the Byrd Subglacial Basin, and the Bentley Subglacial Trench all appear to be underlain by weak rifted lithosphere. The estimated T_e value was found to be insensitive to varying the reference Moho depth between 23 and 27 km and crustal load densities between 2670 and 2800 kg m^{-3}. However, since the best reference Moho depth (23 km) occurs at the low end of this range, we performed further tests by decreasing the minimum reference Moho depth to 18 km. This was found not to alter the best fit T_e value. Regions of higher rigidity may exist within the West Antarctic Rift System; however, if such higher rigidity blocks are relatively localized and bounded by low rigidity zones, it is likely that the entire region will appear to be in local, rather than regional, isostatic equilibrium.

CRUSTAL THICKNESS ESTIMATES

Crustal thickness variations provide key information about the crustal architecture beneath the Pine Island Glacier catchment, which may impact overlying ice dynamics. A continental-scale crustal thickness grid for Antarctica (Müller et al., 2007) has been previously derived from the ice thickness and subglacial topography compiled as part of BEDMAP (Lythe et al., 2000). However, within the catchment of the Pine Island Glacier there is only a single direct estimate of crustal thickness made from receiver function analysis (Winberry and Anandakrishnan, 2004). Our modeling of airborne gravity data is therefore a new tool to assess crustal thickness variations under the West Antarctic Rift System.

There are two key limitations when recovering crustal thickness variations from gravity data. First, intracrustal density contrasts may mask the signal derived from the Moho interface. The effect of such intracrustal bodies must therefore be removed before recovery of Moho undulations. Second, modeling of potential field data is non-unique, and assumptions must therefore be made about both the mean depth of the Moho interface and the density contrast across the Moho.

To estimate Moho variations we used three approaches, which are briefly outlined below; (1) an Airy isostatic model, (2) inversion of the filtered Bouguer gravity anomaly, and (3) inversion of the compensating terrain gravity effect (Fig. 7).

The Airy isostatic model was based solely on the known surface loads (topography and ice thickness) and was used as a reference for the other models, which include observed gravity data. The predicted Moho variations from the Airy isostatic model were low-pass filtered (Fig. 7A), as very short wavelength variations in topography are unlikely to be isostatically supported. The filter we applied passed wavelengths >75 km, cosine tapered wavelengths between 75 and 60 km, and cut off all wavelengths <60 km.

The Bouguer gravity anomaly at long wavelengths is dominated by variations in Moho depth due to isostatic compensation of loads on and within the crust (Watts, 2001). It is therefore often assumed that inversion of the long-wavelength Bouguer anomaly field provides an estimate of Moho depth (Braitenberg et al., 2000; Studinger and Bell, 2007). We therefore applied a low-pass filter (>~75 km for a reference crustal thickness of 35 km) to the Bouguer anomaly to minimize the effect of short-wavelength signals, arising from intracrustal bodies. However, as discussed previously, we assume that a more appropriate reference crustal thickness is 23 km beneath the Pine Island Glacier catchment. This implies that the low-pass filter we applied to the Bouguer anomaly data will attenuate part of the signal from the Moho. Therefore we regard the amplitude of the recovered Moho undulations as a minimum estimate.

Variations in Moho depth (Fig. 7B) were recovered from the long-wavelength Bouguer gravity anomaly using a 3-D inverse modeling approach based on the GLQ method (von Frese et al., 1981). Initial Moho undulations were input and the gravity effect calculated using the GLQ method. The residual between the calculated and observed anomaly was then used to adjust the Moho depth. This process continued iteratively until a good fit (root-mean-square error <3 mGal) between the calculated and the observed gravity anomaly was achieved.

The third approach we utilized is based on inversion of the compensating terrain gravity effect. The "terrain compensating gravity effect" is the difference between the terrain gravity effect and the part of the free-air anomaly that is correlated with the topography. The terrain compensating gravity effect is assumed to be due to isostatic compensation of the surface topography at the Moho (Jones et al., 2002; Braun et al., 2007). The decorrelated part of the free-air anomaly is assumed to be due to intracrustal density variations such as sedimentary basins and igneous intrusions.

To recover the terrain compensating gravity effect we first applied the same low-pass filter used in the Airy isostatic model to both the terrain gravity effect and the free-air gravity anomaly to minimize short wavelength noise. We then used a spectral correlation filter to split the free-air anomaly into two components, one correlated with the topography, and a second decorrelated with the topography. We followed Jones et al. (2002) in assuming that a correlation coefficient of 0.64 excludes the majority of the uncorrelated free-air gravity anomaly.

The Moho undulations derived from the compensating terrain gravity effect (Fig. 7C) were recovered using the method stated previously for the long-wavelength Bouguer gravity anomaly. Our models assumed a reference

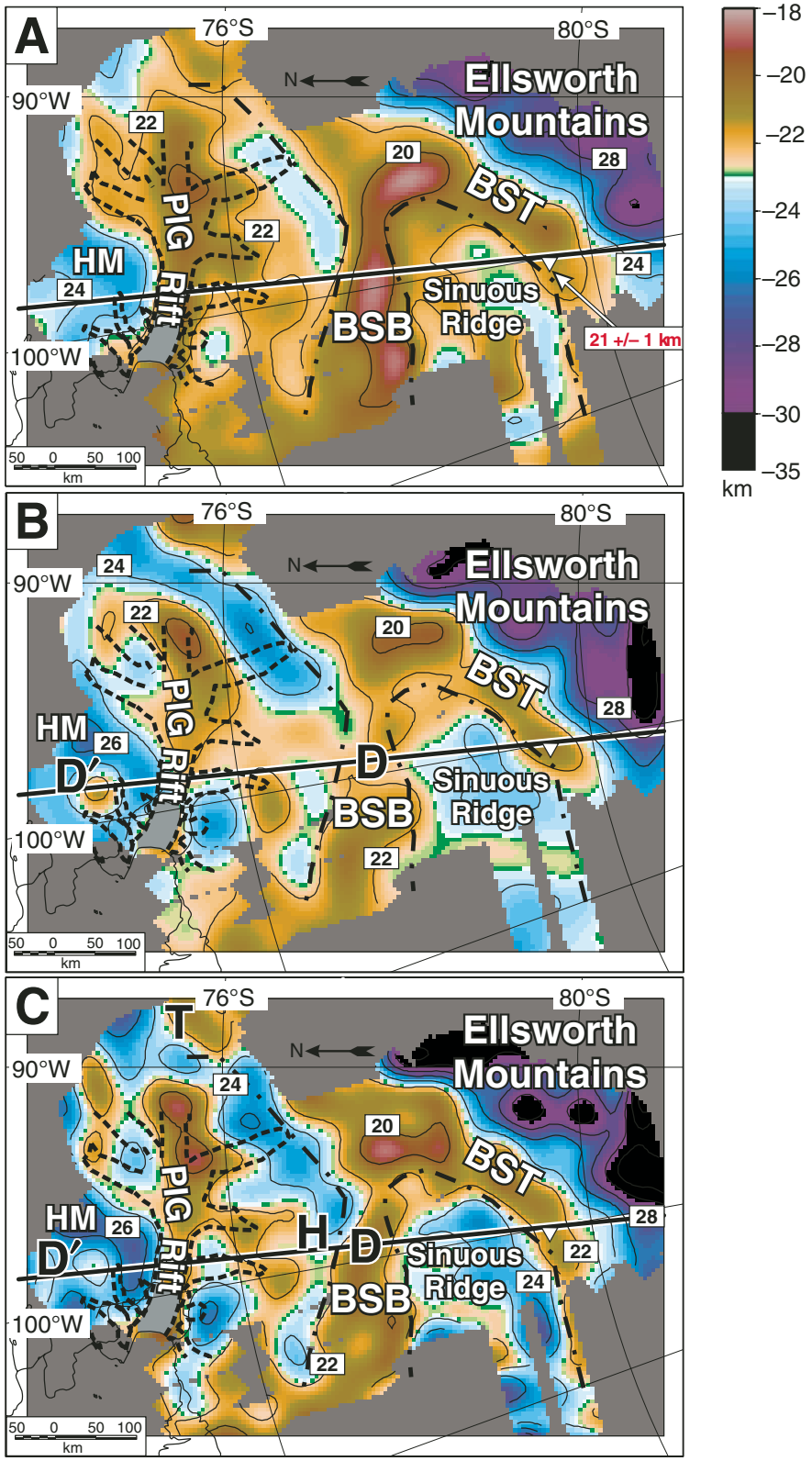

Figure 7. Maps of crustal thickness variation derived from (A) an Airy isostatic model, (B) inversion of long wavelength Bouguer gravity anomaly field, and (C) inversion of the compensating terrain gravity effect. Contour interval = 2 km. Abbreviations: PIG—Pine Island Glacier; BST—Bentley Subglacial Trench; BSB—Byrd Subglacial Basin, HM—Hudson Mountains. Black letters mark features discussed in the text. Other features as in Figure 3A.

Moho depth of 23 km. This yields a crustal thickness of 21 ± 1 km for the Bentley Subglacial Trench, which is consistent with the independent receiver function estimate (Winberry and Anandakrishnan, 2004). For the gravity models Moho depths deeper than the reference depth gave a negative anomaly, and shallower depths gave a positive anomaly. A crust/mantle density contrast of 530 kg m^{-3} and an observation altitude of 2400 m were assumed for all gravity modeling.

Predicted Airy Isostatic Moho Variations

The regional crustal thickness map from the Airy isostatic model suggests crust between 28 and 35 km thick beneath the Ellsworth Mountains and crust over 24 km thick under the Hudson Mountains (Fig. 7A). Narrow linear regions of thinned crust <21 km thick are predicted beneath the Pine Island Glacier graben, Bentley Subglacial Trench, and Byrd Subglacial Basin.

Moho Variation from Filtered Bouguer Gravity Anomaly

Moho predictions based on the filtered Bouguer gravity anomaly exhibit similar patterns to the Airy model (compare Figures 7A and 7B), with thicker crust (>30 km) beneath the Ellsworth Mountains and thinned crust beneath the West Antarctic Rift System. There are, however, regions where the Airy Moho predictions and the pattern from the filtered Bouguer anomaly differ, for example, beneath the Byrd Subglacial Basin (D in Fig. 7B). Here the Airy isostatic model predicts a more linear region of thinner crust compared to the Bouguer derived model. The discrepancy between the Airy isostatic- and Bouguer-derived Moho estimates may be accounted for if several km of low-density sedimentary infill is present in the Byrd Subglacial Basin.

The discrete Moho high (D′) imaged beneath the Hudson Mountains is also likely to be due to contamination of the filtered Bouguer anomaly by an intracrustal source, in this case a mafic intrusion, which is apparent from the Airy isostatic anomaly map (A in Fig. 4B).

Moho Variation from Compensating Terrain Gravity Effect

Depth to Moho estimates recovered from inversion of the compensating terrain gravity effect show an improved match to the predictions of the Airy isostatic model, with a more linear region of shallow Moho observed beneath the Byrd Subglacial Basin (Fig. 7C).

Additionally, the circular shallowing of the Moho in the Hudson Mountains (D′) is attenuated, suggesting a lesser degree of intracrustal contamination. The eastern end of the Pine Island Glacier and under the Byrd Subglacial Basin feature the thinnest crust (~19 ± 1 km). The Bentley Subglacial Trench also appears to be associated with a linear region of thinned crust (21 ± 1 km). The Hudson and Ellsworth Mountains crustal thicknesses are >26 and ~35 km, respectively. The crustal thickness is estimated to be between 23 and 26 km beneath the subglacial highlands (H) separating the Pine Island Glacier from the Byrd Subglacial Basin and beneath the Sinuous Ridge.

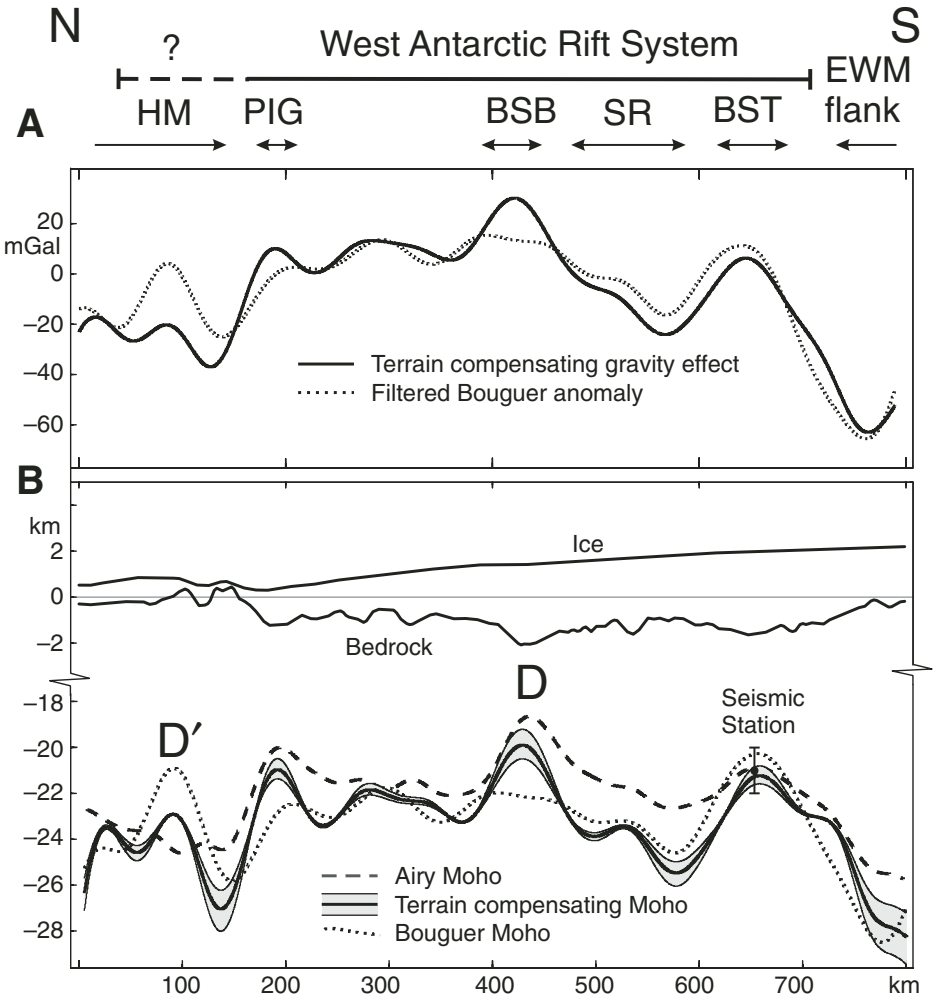

Figure 8. Comparison between crustal thickness estimates derived from the Airy, Bouguer, and terrain compensating methods along the sample profile crossing the West Antarctic Rift System. Panel A shows the input low-pass filtered Bouguer gravity anomaly along the profile and the terrain compensating gravity effect. Panel B shows crustal thickness estimates under the different rift basins. The gray envelope denotes the range of crustal thickness estimates obtained by using the terrain compensating method with different crust/mantle density contrasts (see Table 1). Also note the error bar associated with the receiver function estimate for crustal thickness under the Byrd Subglacial Trench (Winberry and Anandakrishnan, 2004).

Comparison of Techniques

Beneath the Byrd Subglacial Basin and the Hudson Mountains, the filtered Bouguer anomaly method gave significant variations in the Moho pattern, compared to the Airy isostatic model (compare Figures 7B and 7A). We attribute these discrepancies to incomplete removal of intracrustal sources by the low-pass filter. The compensating terrain gravity effect method of Jones et al. (2002) removes intracrustal contamination more effectively and therefore is our preferred method for estimating Moho depth.

There are, however, limitations to inversion of the compensating terrain gravity effect. Intracrustal density contrasts may not always be decorrelated with the surface topography. An example would be sedimentary basins within deep topographic depressions. The correlation of low-density sedimentary infill with low topography will lead to an underestimate of the compensating terrain gravity effect, and hence an underestimate of the amount of crustal thinning. This may be applicable to the Byrd Subglacial Basin, where we have previously identified the presence of possible sedimentary infill. This implies that the crust beneath the Byrd Subglacial Basin may be even thinner than our 19 ± 1 km estimate.

Figure 8 shows a comparison between the different model predictions of Moho depth along our sample profile crossing the West Antarctic Rift System. The most obvious discrepancies between the different Moho depth estimates occur beneath the Pine Island Glacier graben and the Byrd Subglacial Basin. The filtered Bouguer gravity method would yield a broad regional Moho upwarp beneath these basins to depths of ~23 km. The inversion of the compensating terrain gravity effect (our preferred method) indicates more localized regions of thinner crust (19 ± 1 km). All models converge to a Moho depth of 21 ± 1 km under the Bentley Subglacial Trench in good agreement with the independent receiver function estimate (Winberry and Anandakrishnan, 2004).

Sensitivity Tests

The boundary conditions we imposed to account for the non-unique nature of modeling gravity data were a reference Moho depth at 23 km and a density contrast across the Moho of 530 kg m^{-3}. These assumptions will affect the absolute depth and amplitudes of the estimated Moho. However, different physical assumptions do not alter the overall pattern of variation. To assess the impact of increasing the reference Moho depth, or varying the density contrast, we ran several sensitivity tests using the Moho derived from the compensating terrain gravity effect as a reference (Table 1). Increasing the reference Moho depth from 23 to 27 km increases the magnitude of the estimated Moho undulations from ~16 to ~17 km across the entire region. Decreasing the density contrast from 530 to 430 kg m^{-3} had a more significant impact, yielding maximum Moho depths 3 km deeper and minimum Moho

TABLE 1. MINIMUM AND MAXIMUM ESTIMATED MOHO DEPTHS, BASED ON INVERSION OF THE COMPENSATING TERRAIN GRAVITY EFFECT, FOR VARIOUS REFERENCE CRUSTAL THICKNESSES AND DENSITY CONTRASTS ACROSS THE MOHO. BOLD NUMBERS ARE OUR PREFERRED VALUES

Reference crustal thickness (km)	Density contrast (kg m^{-3})	Maximum depth (km)	Minimum depth (km)	Range (km)
23	430	–37.7	–17.7	20.0
23	**530**	**–34.7**	**–18.7**	**16.1**
23	660	–32.3	–19.5	12.8
27	530	–40.8	–23.4	17.3

depths 1 km shallower. In all these tests, the pattern of Moho variation about the reference level remained the same.

DISCUSSION

Crustal Boundaries

The new airborne gravity data collected across the catchment of Pine Island Glacier provides new insights into the crustal structure of the West Antarctic Rift System. The tectonic boundary between the West Antarctic Rift System and the Ellsworth Mountains block is now clearly imaged from the new Bouguer anomaly map (L1 in Fig. 4A). Our interpretation for the Ellsworth Mountains as the uplifted flank of the West Antarctic Rift System would be compatible with apatite-fission track data, which show ~4 km of uplift since the Early Cretaceous (Fitzgerald and Stump, 1991). Crustal thickness beneath the Ellsworth Mountains, as recovered by inversion of the compensating terrain gravity effect, is ~35 km (Fig. 7C). Therefore the crust beneath the Ellsworth Mountains rift flank exhibits comparable thickness to the Whitmore Mountains further to the west (Bell et al., 1999; Studinger et al., 2002) and to the Transantarctic Mountains adjacent to the Ross Sea Rift (Della Vedova et al., 1997; Ferraccioli et al., 2001).

The margin between the West Antarctic Rift System and the Hudson Mountains is less distinct in the new Bouguer gravity anomaly map. The crustal thickness variations recovered from the inversion of the compensating terrain gravity effect (Fig. 7C) reveal a narrow rift zone underlying graben-like topography of the Pine Island Glacier. We name this feature the Pine Island Rift. It is possible that the Pine Island Rift exploited an older inherited tectonic structure, perhaps the southern boundary of the Thurston Island block (Gohl et al., 2007). However, aerogravity data coverage over the Thurston Island block would be necessary to confirm or refute this hypothesis.

Crustal Thinning

Modeling of the new airborne gravity data shows that the crust between the Ellsworth and Hudson Mountains is significantly thinned, indicating that the West Antarctic Rift System extends beneath the catchment of Pine Island Glacier. Predicted Moho depths are between ~26 and ~19 km. The subglacial rifts we imaged follow two distinct trends. The Bentley Subglacial Trench is NE-SW oriented and lies parallel to the Ellsworth Mountains rift flank. In contrast, both the Pine Island Rift and the Byrd Subglacial Basin are approximately E-W oriented and hence lie at a high angle to the West Antarctic Rift flank.

Crustal thickness beneath the catchment of Pine Island Glacier is only slightly higher than the Ross Sea Rift region, where values between 17 and 26 km have been reported (Trey et al., 1999; Bannister et al., 2003). However, sediment thickness in the Ross Sea Rift can reach up to 14 km in the Victoria Land Basin (Brancolini et al., 1995). A comparable thickness of sediments is not present beneath the Pine Island Rift, Bentley Subglacial Basin, or Bentley Subglacial Trench based upon initial depth to magnetic basement estimates (Ferraccioli, 2008, personal commun.), or the single sediment thickness estimate of 550 ± 250 m, derived from receiver function analysis (Anandakrishnan and Winberry, 2004). Between the regions of highly thinned crust we model Moho depths of ~26 km (e.g., beneath the northern part of the Sinuous Ridge), which is similar to the estimated average crustal thickness derived from analysis of airborne gravity data over the West Antarctic Rift System in the Siple Coast region (Studinger et al., 2002). In the northeastern corner of the survey area, a region of thinned crust (T in Fig. 7C) suggests that the West Antarctic Rift System may continue from the Amundsen Sea Embayment toward the Bellingshausen Sea.

Crustal thinning beneath the catchment of the Pine Island Glacier is highly significant since it suggests that elevated geothermal heat flux may occur. If a rifting event occurred relatively recently (<ca. 30 Ma), elevated heat flux would be caused by thinning of the nonconvecting thermal lithosphere (McKenzie, 1967; Nissen et al., 1995) and advection of hot mantle-derived magma into the crust. Mantle-derived magma is likely to give rise to mafic intracrustal intrusions, which would create positive Airy isostatic gravity anomalies such as those we observe (P and P″ in Fig. 4B). Enhanced heat flux associated with crustal thinning processes would be in addition to the regional increase associated with a possible mantle plume beneath the West Antarctic Rift System (Behrendt et al., 1996). Elevated heat flux could provide a source of enhanced basal melting beneath the Amundsen Sea Embayment sector of the West Antarctic Ice Sheet, which would impact on ice dynamics and hence long-term ice-sheet stability (Fahnestock et al., 2001; Parizek et al., 2002).

Crustal Thickness Variations and Inferred Rifting Stages

The range in crustal thicknesses (~19 to ~26 km) we observed under the West Antarctic Rift System between the Ellsworth Mountains and the Hudson Mountains may be explained by inferring two different rifting phases. In this scenario, initial distributed rifting, in the Cretaceous, thinned the crust from ~35 to ~26 km. A later narrower phase of rifting, which we speculate to be Cenozoic in age, caused more localized crustal extension beneath the Pine Island Rift and Byrd Subglacial Basin, where the crust is <20 km thick.

Our gravity-derived interpretation for a two-stage rifting process under the catchment of Pine Island Glacier would be compatible with previous geophysical interpretations for multistage rifting within the Ross Sea segment of the West Antarctic Rift System (Cooper and Davey, 1985; Davey and Brancolini, 1995). Notably, several stages of rifting are observed in many other major continental rift systems worldwide (Olsen, 1995), and different modes of rifting and strain localization (i.e., transitions from wide mode to narrow mode) have been modeled (Benes and Davey, 1996). A two-stage rifting scenario is also compatible with a recent numerical model of rift localization put forward for the Ross Sea Rift region, where a change from distributed to localized rifting within the Victoria Land Basin occurs (Huerta and Harry, 2007).

If a Cenozoic phase of rifting affected the Amundsen Sea Embayment, it may speculatively be linked with spreading within the Adare Trough, which was active between 43 and 26 Ma (Cande et al., 2000). Opening of the Adare Trough may have induced distributed extension within the Ross Sea segment of the West Antarctic Rift System (Decesari et al., 2007). Rotation about the pole suggested by Davey et al. (2006) would induce orthogonal rifting in the Victoria Land Basin, i.e., subparallel to the Transantarctic Mountains, but rifting oblique to the Ellsworth Mountains further to the south. An oblique Cenozoic rifting process may explain the E-W trend of the Pine Island and Byrd

Subglacial Basin rifts, which both run at ~45° to the Ellsworth Mountains rift flank. Alternatively, or additionally, Cenozoic dextral strike-slip motion could have induced oblique rifting beneath the Amundsen Sea segment of the West Antarctic Rift System (Müller et al., 2007).

T_e and Age of Rifting

The observed positive Bouguer gravity anomalies, associated with deep basins within the Pine Island Glacier catchment, are similar in pattern to those detected over the Central Basin of the Ross Sea Rift (Karner et al., 2005). The positive Bouguer anomalies over the Central Basin of the Ross Sea Rift have been explained by postulating that there is a time lag between initial Cretaceous rifting, when the lithosphere was weak (T_e ~0 km), and later Cenozoic sedimentation when the lithosphere had regained its rigidity (T_e ~30 km) (Karner et al., 2005). The increase in rigidity reduces the amount of subsidence at the Moho associated with isostatic compensation of the sedimentary load. The same model has been applied to the Siple Coast region, where positive Bouguer gravity anomaly signatures over the West Antarctic Rift System are associated with major sedimentary basins (Bell et al., 2006). However, Decesari et al. (2007) used subsidence modeling over the Central Basin of the Ross Sea Rift to infer ~40 km of Tertiary extension, thereby questioning the lack of post-Cretaceous extension inferred by Karner et al. (2005).

Under the Pine Island Glacier catchment we have recovered a low rigidity (T_e of 5 ± 5 km) (Fig. 5). Therefore in contrast to previous interpretations over both the Ross Sea and Siple Coast regions, we interpret the positive Bouguer anomalies as arising from isostatic compensation of bedrock topography and ice load. The low T_e over the Amundsen Sea Embayment region could reflect a Cenozoic rifting stage. Alternatively the present-day topography and low T_e could reflect a "fossil" isostatic response to initial Cretaceous rifting. However, the development of a low-relief erosion surface, which has been subsequently uplifted and faulted (LeMasurier and Landis, 1996) argues against the alternative fossil Cretaceous interpretation. The Byrd Subglacial Basin and Bentley Subglacial Trench have recently been interpreted to be young graben-like structures of inferred Neogene age (LeMasurier, 2008). The low T_e values we obtain under the catchment of Pine Island Glacier are similar to other estimates of T_e in active continental rift zones such as ~5 km in the Basin and Range Province (Lowry and Smith, 1994) and are slightly lower than the minimum estimates of ~14 km from the East African Rift system (Tessema and Antoine, 2003).

CONCLUSIONS

We have presented the first airborne gravity images over the catchment of Pine Island Glacier coupled with gravity modeling results. Our analysis provides several new insights into the crustal structure beneath this dynamic part of the West Antarctic Ice Sheet.

(1) The crust under the catchment of Pine Island Glacier has been significantly thinned as a result of continental rifting associated with the West Antarctic Rift System. Crustal thickness is ~35 km under the Ellsworth Mountains rift flank. In contrast, the crust within the rift is between ~26 and 19 km thick. The Byrd Subglacial Basin and the newly identified Pine Island Rift feature the thinnest crust (~19 ± 1 km) observed beneath the West Antarctic Ice Sheet.

(2) Lithospheric rigidity is low (T_e of 5 ± 5 km) under this segment of the West Antarctic Rift System. The low T_e supports the interpretation for an inferred Cenozoic rifting stage that reactivated this segment of the West Antarctic Rift System.

(3) We interpret multiple stages of rifting beneath the Amundsen Sea Embayment. Our interpretation predicts Cretaceous wide mode rifting followed by narrow mode rifting in the Cenozoic. We infer that Cenozoic rifting may provide a source of enhanced heat flow, potentially affecting the dynamics of Pine Island Glacier.

(4) The Byrd Subglacial Basin and the western part of the Pine Island Rift are interpreted to be sedimentary basins, which may enhance glacial flow in the catchment of Pine Island Glacier. In addition we have inferred Cenozoic mafic intrusions, which could represent a local source for elevated heat flow in the Pine Island Glacier region.

ACKNOWLEDGMENTS

We acknowledge support and funding from the Long-Term Survey and Monitoring Programme of the Geological Sciences Division (BAS). We gratefully acknowledge reviewers Wesley LeMasurier and an anonymous reviewer for their constructive advice and their corrections that helped improve the paper significantly. We also thank the associate editor for further suggestions. This paper is a contribution to IPY project (ID No: 107) Geodynamics of the West Antarctic Rift System (WARS) in Remote Ellsworth Land and its implications for the stability of the West Antarctic Ice Sheet. We also wish to acknowledge National Science Foundation grant OPP-0230197 for supporting the fieldwork. We also wish to thank P.T. Leat (BAS) for his advice and comments, which improved upon a draft manuscript.

REFERENCES CITED

Anandakrishnan, S., and Winberry, J.P., 2004, Antarctic subglacial sedimentary layer thickness from receiver function analysis: Global and Planetary Change, v. 42, p. 167–176, doi: 10.1016/j.gloplacha.2003.10.005.

Bannister, S., Yu, J., Leitner, B., and Kennett, B.L.N., 2003, Variations in crustal structure across the transition from West to East Antarctica, Southern Victoria Land: Geophysical Journal International, v. 155, p. 870–884, doi: 10.1111/j.1365-246X.2003.02094.x.

Behrendt, J.C., 1999, Crustal and lithospheric structure of the West Antarctic Rift System from geophysical investigations - a review: Global and Planetary Change, v. 23, p. 25–44, doi: 10.1016/S0921-8181(99)00049-1.

Behrendt, J.C., Saltus, R., Damaske, D., McCaffrey, A., Finn, C., Blankenship, D.D., and Bell, R., 1996, Patterns of Late Cenozoic volcanic and tectonic activity in the West Antarctic Rift System revealed by aeromagnetic surveys: Tectonics, v. 15, p. 660–676, doi: 10.1029/95TC03500.

Bell, R., Blankenship, D.D., Finn, C.A., Morse, D.L., Scambos, T.A., Brozena, J.M., and Hodge, S.M., 1998, Influence of subglacial geology on the onset of a West Antarctic ice stream from aerogeophysical observations: Nature, v. 394, p. 58–62, doi: 10.1038/27883.

Bell, R.E., Childers, V.A., Arko, R.A., Blankenship, D.D., and Brozena, J.M., 1999, Airborne gravity and precise positioning for geologic applications: Journal of Geophysical Research, v. 104, no. B7, p. 15,281–17,292, doi: 10.1029/1999JB900122.

Bell, R., Studinger, M., Karner, G.D., Finn, C., and Blankenship, D., 2006, Identifying major sedimentary basins beneath the West Antarctic Ice Sheet from aeromagnetic data analysis, *in* Fütterer, D.K., et al., eds., Antarctica: Contributions to Global Earth Sciences: Berlin, Springer, p. 117–121.

Benes, V., and Davey, P., 1996, Modes of continental lithospheric extension: Experimental verification of strain localization processes: Earth and Planetary Science Letters, v. 254, p. 69–87.

Blakely, R.J., 1995, Potential Theory in Gravity and Magnetic Applications: Cambridge, Cambridge University Press.

Blankenship, D.D., Bell, R.E., Hodge, S.M., Brozena, J.M., Behrendt, J.C., and Finn, C.A., 1993, Active volcanism beneath the West Antarctic ice sheet and implications for ice-sheet stability: Nature, v. 361, p. 526–529, doi: 10.1038/361526a0.

Braitenberg, C., Zadro, M., Fang, J., Wang, Y., and Hsu, H.T., 2000, The gravity and isostatic Moho undulations in Qinghai-Tibet plateau: Journal of Geodynamics, v. 30, p. 489–505, doi: 10.1016/S0264-3707(00)00004-1.

Brancolini, G., Busetti, M., Marchetti, A., De Santis, L., Zanolla, C., Cooper, A.K., Cochrane, G.R., Zayatz, I., Belyaev, V., Knyazev, M., Vinnikovskaya, O., Davey, F., and Hinz, K., 1995, Descriptive text for the seismic stratigraphic atlas of the Ross Sea, Antarctica, *in* Cooper, A.K., et al., eds., Geology and Seismic Stratigraphy of the Antarctic Margin: Washington, D.C., American Geophysical Union.

Braun, A., Rae Kim, H., Csatho, B., and Von Frese, R.R.B., 2007, Gravity-inferred crustal thickness of Greenland: Earth and Planetary Science Letters, v. 262, p. 138–158, doi: 10.1016/j.epsl.2007.07.050.

Cande, S.C., Stock, J.M., Müller, R.M., and Ishihara, T., 2000, Cenozoic motion between East and West Antarctica: Nature, v. 404, p. 145–150, doi: 10.1038/35004501.

Cape-Roberts-Science-Team, 2000, Studies from the Cape Roberts Project, Ross Sea, Antarctica, Terra Antartica, p. 1–654.

Cooper, A.K., and Davey, F.J., 1985, Marine geological and geophysical investigations in the Ross Sea, Antarctica: Antarctic Journal of the United States, v. 19, p. 80–82.

Corr, H., and Vaughan, D.G., 2008, A recent volcanic eruption beneath the West Antarctic ice sheet: Nature Geoscience, v. 1, p. 122–125, doi:10.1038/ngeo106.

Dalziel, I.W.D., 2006, On the extent of the active West Antarctic Rift System: Terra Antarctica, v. 12, p. 193–202.

Dalziel, I.W.D., and Elliot, D.H., 1982, West Antarctica: Problem child of Gondwanaland: Tectonics, v. 1, p. 3–19.

Dalziel, I.W.D., and Lawver, L., 2001, The lithospheric setting of the West Antarctic Ice Sheet, *in* Alley, R.B., et al., eds., The West Antarctic Ice Sheet: Behavior and Environment, Washington, D.C., American Geophysical Union, p. 29–44.

Damaske, D., Behrendt, J.C., McCaffrey, A., Saltus, R., and Meyer, U., 1994, Transfer faults in the western Ross Sea: New evidence from McMurdo Sound/Ross ice shelf aeromagnetic survey (GANOVEX VI): Antarctic Science, v. 6, p. 359–364, doi: 10.1017/S0954102094000556.

Davey, F.J., and Brancolini, G., 1995, The late Mesozoic and Cenozoic Structural setting of the Ross Sea Region, *in* Cooper, A.K., et al., eds., Geology and Seismic Stratigraphy of the Antarctic Margin: Antarctic Research Series: Washington, D.C., American Geophysical Union, p. 167–182.

Davey, F.J., Cande, S.C., and Stock, J.M., 2006, Extension in the western Ross Sea region-links between Adare Basin and Victoria Land Basin: Geophysical Research Letters, v. 33, 5 p., doi: 10.1029/2006GL027383.

Davis, C.H., Li, Y., McConnell, J.R., Frey, M.M., and Hanna, E., 2005, Snowfall-driven growth in East Antarctic Ice Sheet mitigates recent sea-level rise: Science, v. 308, p. 1898–1901, doi: 10.1126/science.1110662.

Decesari, R.C., Wilson, D.S., Luyendyk, B.P., and Faulkner, M., 2007, Cretaceous and Tertiary extension throughout the Ross Sea, Antarctica, *in* Cooper, A.K., et al., eds., A Keystone in a Changing World – Online Proceedings of the 10th ISAES, Short Research Paper 098, 6 p., doi: 0.3 33/of2007–1047.srp098.

Della Vedova, B., Pellis, G., Trey, H., Zhang, J., Cooper, A.K., Makris, J., and the-ACRUP-working-group, 1997, Crustal structure of the Transantarctic Mountains, Western Ross Sea, *in* Ricci, C.A., ed., The Antarctic Region: Geological evolution and processes: Siena, Terra Antartica Publication, p. 609–618.

Diehl, T.M., Holt, J.W., Blankenship, D.D., Young, D.A., Jordan, T.A., and Ferraccioli, F., 2008, First airborne gravity results over the Thwaites Glacier Catchment, West Antarctica: Geochemistry, Geophysics, Geosystems, 4 p., doi: 10.1029/2007GC001878 (in press).

Fahnestock, M., Abdalati, W., Joughin, I., Brozena, J., and Gogineni, P., 2001, High geothermal heat flow, basal melt, and the origin of rapid ice flow in Central Greenland: Science, v. 294, p. 2338–2342, doi: 10.1126/science.1065370.

Ferraccioli, F., Armadillo, A., Bozzo, E., and Privitera, E., 2000, Magnetics and gravity image tectonic framework of the Mount Melbourne Volcano area (Antarctica): Physics and Chemistry of the Earth, v. 25, no. 4, p. 387–393, doi: 10.1016/S1464-1895(00)00061-2.

Ferraccioli, F., Coren, F., Bozzo, E., Zanolla, C., Gandolfi, S., Tabacco, I.E., and Frezzotti, M., 2001, Rifted crust at the East Antarctic Craton margin; gravity and magnetic interpretation along a traverse across the Wilkes subglacial basin region: Earth and Planetary Science Letters, v. 192, p. 407–421, doi: 10.1016/S0012-821X(01)00459-9.

Ferraccioli, F., Bozzo, E., and Damaske, D., 2002, Aeromagnetic signatures over western Marie Byrd Land provide insight into magmatic arc basement, mafic magmatism and structure of the Eastern Ross Sea Rift flank: Tectonophysics, v. 347, p. 139–165, doi: 10.1016/S0040-1951(01)00242-6.

Ferraccioli, F., Jones, P.C., Curtis, M.L., and Leat, P.T., 2005, Subglacial imprints of early Gondwana breakup as identified from high resolution aerogeophysical data over western Dronning Maud Land, East Antarctica: Terra Nova, v. 17, p. 573–579, doi: 10.1111/j.1365-3121.2005.00651.x.

Ferraccioli, F., Jones, P.C., Vaughan, A.P.M., and Leat, P.T., 2006, New aerogeophysical view of the Antarctic Peninsula: More pieces, less puzzle: Geophysical Research Letters, v. 33, 4 p., doi: 10.1029/2005GL024636.

Ferraccioli, F., Jordan, T.A., Vaughan, D.G., Holt, J.W., James, P.R., Corr, H., Blankenship, D.D., Fairhead, J.D., and Diehl, T.M., 2007, New aerogeophysical survey targets the extent of the West Antarctic Rift System over Ellsworth Land, *in* Cooper, A.K., et al., eds., Antarctica: A Keystone in a Changing World –Online Proceedings of the 10th ISAES X, USGS, p. 4.

Fielding, C., Henrys, S.A., and Wilson, T.J., 2006, Rift history of the western Victoria Land Basin: A new perspective based on integration of cores with seismic reflection data, *in* Futterer, D.K., et al., eds., Antarctica: Contributions to Global Earth Sciences: Berlin, Springer-Verlag, p. 307–316.

Finn, C., Dietmar-Müller, R., and Panter, K.S., 2005, A Cenozoic diffuse alkaline magmatic province (DAMP) in the southwest Pacific without rift or plume origin: Geochemistry, Geophysics, Geosystems, v. 6, 26 p., doi: 10.1029/2004GC000723.

Fitzgerald, P.G., and Stump, E., 1991, Early Cretaceous uplift in the Ellsworth Mountains of West Antarctica: Science, v. 254, p. 92–94, doi: 10.1126/science.254.5028.92.

Gohl, K., Tererin, D., Eagles, G., Netzeband, G., Grobys, J.W.G., Parsiegla, N., Schlüter, P., Leinweber, V., Larter, R.D., Uenzelmann-Neben, G., and Udintsev, G.B., 2007, Geophysical survey reveals tectonic structures in the Amundsen Sea embayment, West Antarctica, *in* Cooper, A.K., et al., eds., Antarctica: A Keystone in a Changing World – Online Proceedings of the 10th ISAES, USGS Open-File Report, doi:10.3133/of2007-1047.srp047.

Harlan, R.B., 1968, Eotvos corrections for airborne gravity: Journal of Geophysical Research, v. 73, p. 4675–4679, doi: 10.1029/JB073i014p04675.

Holt, J.W., Blankenship, D.D., Morse, D.L., Young, D.A., Peters, M.E., Kempf, S.D., Richter, T.G., Vaughan, A.P.M., and Corr, H., 2006a, New boundary conditions for the West Antarctic Ice Sheet: Subglacial topography of the Thwaites and Smith Glacier Catchments: Geophysical Research Letters, v. 33, 4 p., doi: 10.1029/2005GL025561.

Holt, J.W., Richter, T.G., Kempf, S.D., and Morse, D.L., 2006b, Airborne gravity over Lake Vostok and adjacent highlands of East Antarctica: Geochemistry, Geophysics, Geosystems, v. 7, no. 11, 15 p., doi: 10.1029/2005GC001177.

Huerta, A.D., and Harry, D.L., 2007, The transition from diffuse to focused extension: Modeled evolution of the West Antarctic Rift system: Earth and Planetary Science Letters, v. 255, p. 133–147, doi: 10.1016/j.epsl.2006.12.011.

Hulbe, C.L., and MacAyeal, D.R., 1999, A new numerical model of coupled inland ice sheet, ice stream, and ice shelf flow and its application to the West Antarctic Ice Sheet: Journal of Geophysical Research, v. 104, p. 349–366, doi: 10.1029/1999JB900264.

Jones, P.C., and Ferris, J.K., 1999, Short note: A new estimate of the adopted gravity value at Rothera Station, Antarctic Peninsula: Antarctic Science, v. 11, p. 461–462, doi: 10.1017/S0954102099000590.

Jones, P.C., and Johnson, A.C., 1995, Airborne gravity survey in southern Palmer Land, Antarctica, *in* Proceedings of IAG Symposium on Airborne Field Determination, IUGG XXI General Assembly, Boulder, Colorado, p. 117–123.

Jones, P.C., Johnson, A.C., von Frese, R.R.B., and Corr, H., 2002, Detecting rift basins in the Evans Ice Stream region of West Antarctica using airborne gravity data: Tectonophysics, v. 347, p. 25–41, doi: 10.1016/S0040-1951(01)00236-0.

Jordan, T.A., Ferraccioli, F., Corr, H., Robinson, C., Caneva, G., Armadillo, A., Bozzo, E., and Frearson, N., 2007, Linking the Wilkes Subglacial Basin, the Transantarctic Mountains, and the Ross Sea with a new airborne gravity survey: Terra Antartica Reports, v. 13, p. 18.

Karner, G.D., Studinger, M., and Bell, R., 2005, Gravity anomalies of sedimentary basins and their mechanical implications: Application to the Ross Sea basins, West Antarctica: Earth and Planetary Science Letters, v. 235, p. 577–596, doi: 10.1016/j.epsl.2005.04.016.

LaCoste, L.J.B., 1967, Measurement of gravity at sea and in the air: Reviews of Geophysics, v. 5, no. 4, p. 477–526, doi: 10.1029/RG005i004p00477.

Larter, R.D., Cunningham, A.P., and Barker, P.F., 2002, Tectonic evolution of the Pacific margin of Antarctica 1. Late Cretaceous tectonic reconstructions: Journal of Geophysical Research, v. 107, no. B12, 19 p., doi: 10.1029/2000JB000052.

Lawver, L., and Gahagan, L.M., 1994, Constraints on timing of extension in the Ross Sea region: Terra Antartica Reports, v. 1, p. 545–552.

LeMasurier, W.E., 2008, Neogene extension and basin deepening in the West Antarctic rift inferred from comparisons with the East African rift and other analogs: Geology, v. 36, p. 247–250, doi: 10.1130/G24363A.1.

LeMasurier, W.E., and Landis, C.A., 1996, Mantle-plume activity recorded by low-relief erosion surfaces in West Antarctica and New Zealand: Geological Society of America Bulletin, v. 108, p. 1450–1466, doi: 10.1130/0016-7606(1996)108<1450:MPARBL>2.3.CO;2.

LeMasurier, W.E., and Thomson, J.W., 1990, Volcanoes of the Antarctic Plate and Southern Oceans, Antarctic Research Series: Washington, D.C., American Geophysical Union, p. 512.

Liu, H., Jezek, K., Li, B., and Zhao, Z., 2001, Radarsat Antarctic Mapping Project digital elevation model version 2: Boulder, Colorado, National Snow and Ice Data Center, digital media.

Lowry, A.R., and Smith, R.B., 1994, Flexural rigidity of the Basin and Range-Colorado Plateau-Rocky Mountains transition from coherence analysis of gravity and topography: Journal of Geophysical Research, v. 99, p. 20,123–20,140, doi: 10.1029/94JB00960.

Luyendyk, B.P., 1995, Hypothesis for Cretaceous rifting of east Gondwana caused by subducted slab capture: Geology, v. 23, p. 373–376, doi: 10.1130/0091-7613(1995)023<0373:HFCROE>2.3.CO;2.

Lythe, M.B., Vaughan, D.G., and the-BEDMAP-Consortium, 2000, BEDMAP – bed topography of the Antarctic: British Antarctic Survey.

Mader, G.L., 1992, Rapid static and kinematic global positioning system solutions using the ambiguity function technique: Journal of Geophysical Research, v. 97, p. 3271–3283, doi: 10.1029/91JB02845.

McKenzie, D.P., 1967, Some remarks on heat flow and gravity anomalies: Journal of Geophysical Research, v. 72, p. 6261–6271, doi: 10.1029/JZ072i024p06261.

Mukasa, S.B., and Dalziel, I.W.D., 2000, Marie Byrd Land, West Antarctica: Evolution of Gondwana's Pacific margin constrained by zircon U-Pb geochronology and feldspar common-Pb isotopic compositions: Geological Society of America Bulletin, v. 112, p. 611–627, doi: 10.1130/0016-7606(2000)112<0611:MBLWAE>2.3.CO;2.

Müller, R.M., Cande, S.C., Stock, J.M., and Keller, W.R., 2005, Crustal structure and rift flank uplift of the Adare Trough, Antarctica: Geochemistry, Geophysics, Geosystems, v. 6, 16 p., doi: 10.1029/2005GC001027.

Müller, R.M., Gohl, K., Cande, S.C., Goncharov, A., and Golynsky, A.V., 2007, Eocene to Miocene geometry of the West Antarctic Rift System: Australian Journal of Earth Sciences, v. 54, p. 1033–1045, doi: 10.1080/08120090701615691.

Nissen, S.S., Hayer, D.E., Bochu, Y., Weijun, Z., Yongqin, C., and Xiaupin, X., 1995, Gravity, heat flow, and seismic constraints on the processes of crustal extension: Northern margin of the South China Sea: Journal of Geophysical Research, v. 100, p. 22,447–22,483, doi: 10.1029/95JB01868.

Olsen, K.H., 1995, Continental rifts: Evolution, structure, tectonics (Developments in geotectonics), New York, Elsevier Science, 490 p.

Parizek, B.R., Alley, R.B., Anandakrishnan, S., and Conway, H., 2002, Subcatchment melt and long term stability of ice stream D, West Antarctica: Geophysical Research Letters, v. 29, 4 p., doi: 10.1029/2001GL014326.

Rignot, E.J., 1998, Fast recession of a West Antarctic Glacier: Science, v. 281, p. 549–551, doi: 10.1126/science.281.5376.549.

Rignot, E.J., Thomas, R., Kanagaratnam, P., Casassa, G., Frederick, E., Gogineni, S., Krabill, W., Rivera, A., Russell, R., Sonntag, J., Swift, R., and Yungel, J., 2004, Improved estimation of the mass balance of glaciers draining into the Amundsen Sea sector of West Antarctica from the CECS/NASA 2002 campaign: Annals of Glaciology, v. 39, p. 231–237, doi: 10.3189/172756404781813916.

Rignot, E.J., Bamber, J.L., Van Den Broeke, M.R., Davis, C., Li, Y., Van De Berg, W.J., and Van Meijgaard, E., 2008, Recent Antarctic ice mass loss from radar interferometry and regional climate modelling: Nature Geoscience, v. 1, p. 106–110, doi: 10.1038/ngeo102.

Rocchi, S., Armienti, P., D'Orazio, M., Tonarini, S., Wijbrans, J.R., and Di Vincenzo, G., 2002, Cenozoic magmatism in the western Ross Embayment: Role of mantle plume

versus plate dynamics in the development of the West Antarctic Rift System: Journal of Geophysical Research, v. 107, 22 p., doi:10.1029/2001JB000515.

Rocchi, S., LeMasurier, W.E., and Di Vincenzo, G., 2006, Oligocene to Holocene erosion and glacial history in Marie Byrd Land, West Antarctica, inferred from exhumation of the Dorrel Rock intrusive complex and from volcano morphologies: GSA Bulletin, v. 118, doi: 10.1130/B25675.1.

Sasagawa, G., Meunier, T.K., Mullins, J.L., McAdoo, D., and Klopping, F., 2004, Absolute Gravimetry in Antarctica: 1995 observations at McMurdo Station and Terra Nova Bay Station: Open-File report 2004–1190, 49 p.

Shepherd, A., Wingham, D., and Rignot, E.J., 2004, Warm ocean is eroding West Antarctic Ice Sheet: Geophysical Research Letters, v. 31, 4 p., doi: 10.1029/2004GL021106.

Siddoway, C.S., Richard, S., Fanning, C.M., and Luyendyk, B.P., 2004, Origin and emplacement mechanisms for a middle Cretaceous gneiss dome, Fosdick Mountains, West Antarctica, *in* Whitney, D.L., et al., eds., Gneiss domes in orogeny, Geological Society of America Special Paper 380, p. 267–294.

Siddoway, C.S., Sass, L.C.I., and Esser, R., 2005, Kinematic history of the Marie Byrd Land terrane, West Antarctica: Direct evidence from Cretaceous mafic dykes, *in* Vaughan, A.P.M., et al., eds., Terrane processes at the margin of Gondwana: Special Publication Geological Society of London 246, p. 417–438.

Smith, W.H.F., and Wessel, P., 1990, Gridding with continuous curvature splines in tension: Geophysics, v. 55, p. 293–305, doi: 10.1190/1.1442837.

Steinberger, B., Sutherland, R., and O'Connell, J., 2004, Prediction of Emperor-Hawaii seamount locations from a revised model of global plate motion and mantle flow: Nature, v. 430, p. 167–173, doi: 10.1038/nature02660.

Stewart, J., and Watts, A.B., 1997, Gravity anomalies and spatial variations of flexural rigidity at mountain ranges: Journal of Geophysical Research, v. 102, p. 5327–5352, doi: 10.1029/96JB03664.

Storey, B.C., Leat, P.T., Weaver, S.D., Pankhurst, R.J., Bradshaw, J.D., and Kelley, S., 1999, Mantle plumes and Antarctica-New Zealand rifting; evidence from mid-Cretaceous mafic dykes: Journal of the Geological Society, v. 156, p. 659–671, doi: 10.1144/gsjgs.156.4.0659.

Studinger, M., and Bell, R., 2007, Moho topography of the West Antarctic Rift System from inversion of aerogravity data: Ramifications for geothermal heat flux and ice streaming, *in* Cooper, A.K., et al., eds., Antarctica: A Keystone in a Changing World—Online Proceedings of the 10th ISAES X, USGS Open-File Report 2007–1047, extended abstract 031.

Studinger, M., Bell, R., Finn, C.A., and Blankenship, D.D., 2002, Mesozoic and Cenozoic extensional tectonics of the West Antarctic Rift System from high-resolution airborne geophysical mapping: Royal Society of New Zealand Bulletin, v. 35, p. 563–569.

Swain, C.J., 1996, Horizontal acceleration corrections in airborne gravimetry: Geophysics, v. 61, p. 273–276, doi: 10.1190/1.1443948.

Tessema, A., and Antoine, L.A.G., 2003, Variation in effective elastic plate thickness of the East Africa lithosphere: Journal of Geophysical Research, v. 108, 16 p., doi:10.1029/2002JB002200.

Thomas, R., Rignot, E.J., Casassa, G., Kanagaratnam, P., Acuña, C., Akins, T., Brecher, H., Frederick, E., Gogineni, P., Krabill, W., Manizade, S., Ramamoorthy, H., Rivera, A., Russell, R., Sonntag, J., Swift, R., Yungel, J., and Zwally, J., 2004, Accelerated Sea-Level Rise from West Antarctica: Science, v. 306, p. 255–258, doi: 10.1126/science.1099650.

Trey, H., Cooper, A.K., Pellis, G., Della Vedova, B., Cochrane, G., Brancolini, G., and Makris, J., 1999, Transect across the West Antarctic rift system in the Ross Sea, Antarctica: Tectonophysics, v. 301, p. 61–74, doi: 10.1016/S0040-1951(98)00155-3.

Valliant, H.D., 1992, LaCoste & Romberg Air/Sea Meters: An Overview, CRC Handbook of Geophysical Exploration at Sea: London, CRC Press.

Vaughan, D.G., Corr, H., Ferraccioli, F., Frearson, N., O'Hare, A., Mach, D., and Holt, J.W., 2006, New boundary conditions for the West Antarctic Ice Sheet: Subglacial topography beneath Pine Island Glacier: Geophysical Research Letters, v. 33, 4 p., doi:10.1029/2005GL025588.

Vogel, S.W., and Tulaczyk, S., 2006, Ice-dynamical constraints on the existence and impact of subglacial volcanism on West Antarctic ice sheet stability: Geophysical Research Letters, v. 33, 4 p., doi: 23510.21029/22006GL027345.

von Frese, R.R.B., Hinze, W.J., Braile, L.W., and Luca, A.J., 1981, Spherical earth gravity and magnetic anomaly modeling by Gauss- Legendre quadrature integration: Journal of Geophysics, v. 49, p. 234–242.

Wannamaker, P.E., Stodt, J.A., and Olsen, S.L., 1996, Dormant state of rifting below the Byrd Subglacial Basin, West Antarctica, implied by magnetotelluric (MT) profiling: Geophysical Research Letters, v. 23, p. 2983–2986, doi: 10.1029/96GL02887.

Watts, A.B., 2001, Isostasy and flexure of the lithosphere: Cambridge, Cambridge University Press, 458 p.

Weaver, S.D., Storey, B.C., Pankhurst, R.J., Mukasa, S.B., DiVenere, V.J., and Bradshaw, J.D., 1994, Antarctica-New Zealand rifting and Marie Byrd Land lithospheric magmatism linked to ridge subduction and mantle plume activity: Geology, v. 22, p. 811–814, doi: 10.1130/0091-7613(1994)022<0811:ANZRAM>2.3.CO;2.

Wessel, P., and Smith, W.H.F., 1991, Free software helps map and display data: Eos, Transactions, American Geophysical Union, v. 72, p. 441, doi: 10.1029/90EO00319.

Winberry, J.P., and Anandakrishnan, S., 2003, Seismicity and neotectonics of West Antarctica: Geophysical Research Letters, v. 30, 3 p., doi:10.1029/2003GL018001.

Winberry, J.P., and Anandakrishnan, S., 2004, Crustal structure of the West Antarctic rift system and Marie Byrd Land hotspot: Geology, v. 32, p. 977–980, doi: 10.1130/G20768.1.

Woollard, G.P., 1979, The new gravity system—Changes in international gravity base values and anomaly values: Geophysics, v. 44, p. 1352–1366, doi: 10.1190/1.1441012.

Manuscript Received 18 February 2008
Revised Manuscript Received 22 October 2008
Manuscript Accepted 23 April 2009

Printed in the USA